RF-Driven Josephson Bifurcation Amplifier for Quantum Measurement

I. Siddiqi, R. Vijay, F. Pierre, C. M. Wilson, M. Metcalfe, C. Rigetti, L. Frunzio, and M. H. Devoret

Departments of Applied Physics and Physics, Yale University, New Haven, Connecticut 06520-8284, USA

(Received 11 February 2004; published 10 November 2004)

We have constructed a new type of amplifier whose primary purpose is the readout of superconducting quantum bits. It is based on the transition of a rf-driven Josephson junction between two distinct oscillation states near a dynamical bifurcation point. The main advantages of this new amplifier are speed, high sensitivity, low backaction, and the absence of on-chip dissipation. Pulsed microwave reflection measurements on nanofabricated Al junctions show that actual devices attain the performance predicted by theory.

DOI: 10.1103/PhysRevLett.93.207002 PACS numbers: 85.25.Cp, 05.45.–a

Quantum measurements of solid-state systems, such as the readout of superconducting quantum bits [1–7], challenge conventional low-noise amplification techniques. Ideally, the amplifier for a quantum measurement should minimally perturb the measured system while maintaining sufficient sensitivity to overcome the noise of subsequent elements in the amplification chain. Additionally, the drift of materials properties in solid-state systems mandates a fast acquisition rate to permit measurements in rapid succession. To meet these inherently conflicting requirements, we propose to harness the sensitivity of a dynamical system—a single rf-driven Josephson tunnel junction—tuned near a bifurcation point. In this new scheme, all available degrees of freedom in the dynamical system participate in information transfer and none contribute to unnecessary dissipation resulting in excess noise. The superconducting tunnel junction is the only electronic circuit element that remains nonlinear and nondissipative at arbitrary low temperatures. As the key component of present superconducting amplifiers [8–10], it is known to exhibit a high degree of stability.

The operation of our Josephson bifurcation amplifier (JBA) is represented schematically in Fig. 1. The central element is a Josephson junction whose critical current I_0 is modulated by the input signal using an application-specific coupling scheme, such as a SQUID loop (see inset of Fig. 1) or a superconducting single-electron transistor (SSET) like in superconducting charge qubits (input port). The junction is driven with a sinusoidal signal $i_{\rm rf}\sin(\omega t)$ fed from a transmission line through a circulator (drive port). In the underdamped regime, when the drive frequency ω is detuned from the natural oscillation frequency ω_p, the system can have two possible oscillation states that differ in amplitude and phase [11,12]. Starting in the lower amplitude state, at the bifurcation point $i_{\rm rf} = I_B \ll I_0$, the system becomes infinitely sensitive, in absence of thermal and quantum fluctuations, to variations in I_0. At finite temperature, sensitivity scales as $k_B T/\varphi_0$, where $\varphi_0 = \hbar/2e$ is the reduced flux quantum and T the temperature. The reflected component of the drive signal, measured through another transmission line connected to the circulator (output port), is a convenient signature of the junction oscillation state that carries with it information about the input signal. This arrangement minimizes the backaction of the amplifier since the only fluctuations felt at its input port arise from the load impedance of the circulator, which is physically separated from the junction via a transmission line of arbitrary length and can therefore be thermalized efficiently to base temperature. In this Letter, we present an experiment that demonstrates the principle of bifurcation amplification.

The dynamics of the junction are described by the time evolution of the junction gauge-invariant phase difference $\delta(t) = \int_{-\infty}^{t} dt' 2eV(t')/\hbar$, where V is the voltage across the junction. In presence of the microwave drive $i_{\rm rf}\sin(\omega t)$, the oscillations of the junction phase can be parameterized using in-phase and quadrature-phase components $\delta(t) = \delta_{\parallel}\sin(\omega t) + \delta_{\perp}\cos(\omega t)$ (higher harmonics of oscillation are negligible). When the detuning $\alpha = (1 - \omega/\omega_p)$ and the quality factor $Q = \omega_p RC$ satisfy $\alpha Q > \sqrt{3}/2$, then two steady-state solutions can exist for $\delta(t)$ (see Fig. 2). Here $\omega_p = (2eI_0/\hbar C)^{1/2}$ is the junc-

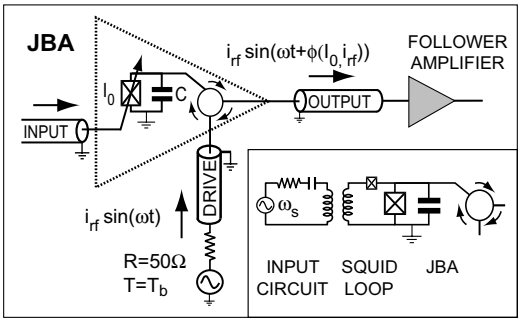

FIG. 1. Schematic diagram of the Josephson bifurcation amplifier. A junction with critical current I_0, parametrically coupled to the input port, is driven by a rf signal which provides the power for amplification. In the vicinity of the dynamical bifurcation point $i_{\rm rf} = I_B$, the phase of the reflected signal phase ϕ depends critically on the input signal. Inset: example of a parametric input coupling circuit.

tion plasma frequency, C is the capacitance shunting the Josephson element, and $R = 50\ \Omega$ is the characteristic impedance of the transmission line at the output and drive ports. Figure 2 has been calculated for $\alpha = 0.122$, $Q = 20$, and $i_{\rm rf}/I_B = 0.87$, where $I_B = 16/(3\sqrt{3}) \times \alpha^{3/2}(1-\alpha)^{3/2} I_0 + O[1/(\alpha Q)^2]$. These values correspond to operating conditions for measurements described below. The dynamical switching from state 0 to 1 is characterized by a phase shift given here by $\tan^{-1}[(\delta_{\|}^1 - \delta_{\|}^0)/(\delta_{\perp}^1 - \delta_{\perp}^0)] = -139$ deg. Using the junction phase-voltage relationship and the transmission line equations, we can calculate the steady-state magnitude and phase of the reflected microwave drive signal. The change in the oscillation of δ results in a shift of the reflected signal phase $\Delta\phi_{01} = 89$ deg. (In very recent experiments, we have been able to optimize parameters and achieve $\Delta\phi_{01} = 180$ deg.) Since there is no source of dissipation in the junction chip, there should be no change in the magnitude of the reflected signal power, even though $\sqrt{(\delta_{\|}^1 - \delta_{\|}^0)^2 + (\delta_{\perp}^1 - \delta_{\perp}^0)^2} \neq 0$.

Our sample consisted of a single shadow-mask evaporated $Al/Al_2O_3/Al$ tunnel junction with $I_0 = 1.17\ \mu$A, shunted with an on-chip lithographic capacitance $C =$ 27.3 pF [12] to obtain a reduced plasma frequency $\omega_p/2\pi = 1.80$ GHz. The dynamics of the transition between the two oscillation states were probed using microwave pulses, generated by the amplitude modulation of a cw source with a phase-locked arbitrary waveform generator with 1 ns resolution. The reflected signal was passed through a circulator at base temperature $T = 0.25$ K to a matched high electron mobility transistor (HEMT) amplifier at $T = 4.2$ K. At room temperature, the reflected signal was further amplified, mixed down to 100 MHz and finally digitally demodulated using a 2 GS/s digitizer to extract the signal phase ϕ.

We first probed the drive current dependence of the reflected signal phase $\phi(i_{\rm rf})$ by applying a 4 μs long symmetric triangular shaped pulse with a peak value $0.185 I_0$. The demodulated reflected signal was divided into 20 ns sections, each yielding one measurement of ϕ for a corresponding value of $i_{\rm rf}$. The measurement was repeated 6×10^5 times to obtain a distribution of $\phi(i_{\rm rf})$. In Fig. 3, the mode of the distribution is plotted as a function of $i_{\rm rf}/I_0$. For $i_{\rm rf}/I_0 < 0.125$, the bifurcation amplifier is always in state 0 and ϕ is constant and assigned a value of 0 deg. As the drive current is increased above $i_{\rm rf}/I_0 = 0.125$, thermal fluctuations are sufficiently large to cause transitions to the 1 state. In the region between the two dashed lines at $i_{\rm rf}/I_0 = 0.125$ and $i_{\rm rf}/I_0 = 0.160$, ϕ displays a bimodal distribution with peaks centered at 0 and 74 deg with the latter corresponding to the amplifier in the 1 state, as we have demonstrated previously [12]. The dotted line in Fig. 3 is the average reflected signal phase $\langle\phi\rangle$. When $i_{\rm rf}/I_0$ is increased above 0.160, the system is only found in state 1. In the decreasing part of the $i_{\rm rf}$ ramp, the system does not start to switch back to state 0 until $i_{\rm rf}/I_0 = 0.065$. The critical switching cur-

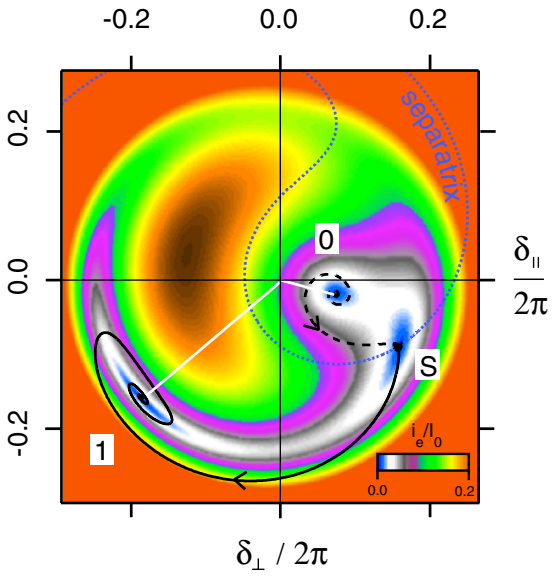

FIG. 2 (color online). Poincaré section of a rf-driven Josephson junction in the bistable regime [$\alpha = (1 - \omega/\omega_p) = 0.122$, $i_{\rm rf}/I_B = 0.87$]. The coordinates $\delta_{\|}$ and $\delta_{\perp}$ are the in-phase and quadrature-phase components of the junction gauge-invariant phase difference δ. The color code gives the magnitude of the error current i_e [18], which describes the "force" on δ. The two stable oscillation states, labeled by 0 and 1, are indicated by white line segments. The basins of attraction corresponding to the two states are separated by the blue dotted line (separatrix). Point S, which lies on the separatrix, is the saddle point at which the escape trajectory from state 0 (dashed line) meets the retrapping trajectory into state 1 (solid line).

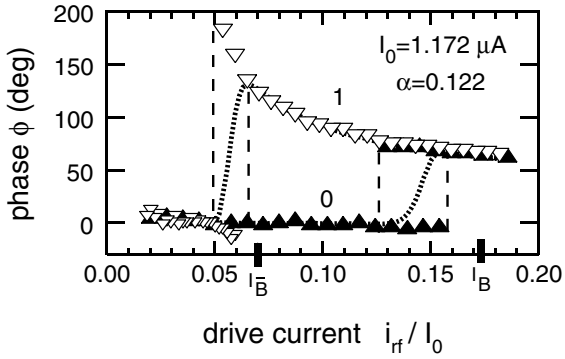

FIG. 3. Hysteretic variation of the reflected signal phase ϕ with drive current $i_{\rm rf}/I_0$. Symbols denote the mode of ϕ, with up and down triangles corresponding to increasing and decreasing $i_{\rm rf}$, respectively. The dotted line is $\langle\phi\rangle$. The calculated bifurcation points, $I_{\bar{B}}$ and I_B, are marked on the horizontal axis. The 0 and 1 phase states are reminiscent of the superconducting and dissipative states of the dc current-biased junction.

rents I_B for the $0 \rightarrow 1$ transition and $I_{\bar{B}}$ for the $1 \rightarrow 0$ transition, calculated from numerical simulations to treat the inductance of wire bonds, are denoted with ticks in Fig. 3, and are in good agreement with experiment. The $0 \rightarrow 1$ transition at $i_{\mathrm{rf}} = I_B$ is nearly irreversible, allowing the bifurcation amplifier to latch and store its output during the integration time set by the sensitivity of the follower amplifier.

We have then characterized the switching phenomenon in the vicinity of the $0 \rightarrow 1$ transition. The drive current was ramped from 0 to its maximum value in 40 ns and was then held constant at a plateau for 40 ns before returning to 0. Only the final 20 ns of the signal in the plateau were analyzed to determine the oscillation phase, the first 20 ns being allotted for settling of the phase. Histograms taken at an acquisition rate of 10 MHz are shown in Fig. 4. The 0 and 1 peaks can easily be resolved with a small relative overlap of 10^{-2}. We have also "latched" the state of the amplifier by reducing the drive amplitude of the analysis plateau by 20% relative to the settling plateau. Now, by increasing the analysis time to 300 ns, the overlap was reduced to 6×10^{-5}.

The switching probability $P_{0\rightarrow1}(i_{\mathrm{rf}})$, i.e., the weight of the 1 peak in Fig. 4, was measured for different values of the temperature T and I_0, the latter being varied with a magnetic field applied parallel to the junction plane (see Fig. 5). Defining the discrimination power d as the maximum difference between two switching probability curves that differ in I_0, we find that at $T = 340$ mK, $d = 57\%$ for $\Delta I_0/I_0 = 1\%$—the typical variation between qubit states in a "quantronium" circuit [2], which is in essence a SSET coupled to a readout junction operated in dc switching mode. The switching probability curves should shift according to $(\Delta I_B/I_B)/(\Delta I_0/I_0) = 3/(4\alpha) - 1/2 + O[1/(\alpha Q)^2]$, which for our case takes the value 5.6. In Fig. 5, the curves are shifted by 6%, which agrees well with this prediction. For the case of the dc current-biased junction, similar curves would shift only by 1% since the switching current is I_0 itself. Comparable discrimination power using dc switching has only been achieved in these devices at $T \lesssim 60$ mK. As the temperature is increased, the switching probability curves broaden due to increased thermal fluctuations and the discrimination power decreases: at $T = 540$ mK, $d = 49\%$. With improved rf filtering and a more optimized sample, we reached $T = 250$ mK and obtained $d = 80\%$. This temperature dependence of the discrimination power is in agreement with both analytical predictions and independent measurement of the rate of escape out of the dynamical well (data not shown). The temperatures quoted above are inferred from the measured escape rate and calculated barrier heights using the method of Ref. [13].

With the Josephson bifurcation amplifier operating at $T = 340$ mK, it is possible to resolve with a signal/noise ratio of 1 a 10 nA variation in I_0 in a total time $\tau \lesssim 80$ ns, corresponding to a critical current sensitivity of $S_{I_0}^{1/2} = 3.3 \times 10^{-12}$ A/Hz$^{1/2}$. This value is in agreement with the analytical theory prediction $S_{I_0}^{1/2} = \eta(i_{\mathrm{rf}}/I_0, \alpha) \times (k_B T/\varphi_0) \cdot \tau^{1/2}$, where $\eta \approx 1.4$ near the bifurcation point. Dispersive readout in the linear regime has been proposed [14] on account of its minimal effect on qubit coherence and relaxation. Increasing the drive amplitude near the dynamical bifurcation has the further benefit, for a given Q, of maximizing the phase shift between the two qubit states and thus eliminating any loss of fidelity due to noise of the follower amplifier.

The JBA can also be operated in the nonhysteretic regime when $\alpha Q \lesssim \sqrt{3}/2$. In this mode, it is straightforward to define conventional amplifier quantities such as power gain and noise temperature, thus allowing direct comparison with other ultra-low-noise amplifiers such as the SQUID [15]. With the model shown in the inset of Fig. 1, and assuming that the modulation of drive signal has symmetric sidebands, we calculate the power gain and the noise temperature to be $2\omega_p/\omega_s$ and $\hbar\omega_s/k_B$, respectively, where ω_s is the input signal frequency. We

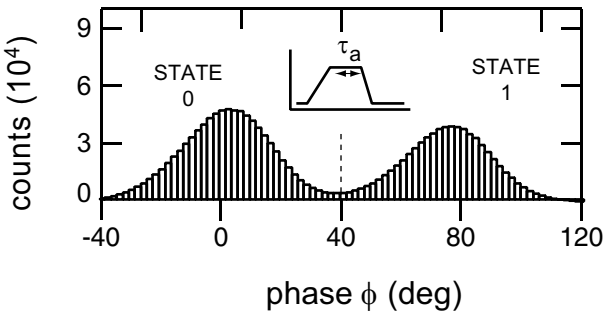

FIG. 4. Histograms of the reflected signal phase ϕ at $i_{\mathrm{rf}}/I_0 = 0.145$. The histogram contains 1.6×10^6 counts with an analysis time $\tau_a = 20$ ns. Data here have been taken under the same operating conditions as in Fig. 3. The dashed line represents the discrimination threshold between the 0 and 1 state.

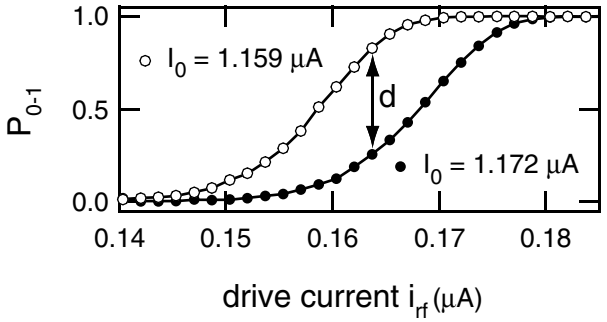

FIG. 5. Switching probability curves at $T = 340$ mK as a function of the drive current i_{rf}. The discrimination power $d = 0.57$ is the maximum difference between the two curves. The measurement protocol is the same as shown in the upper panel of Fig. 4. Though the two curves differ by approximately 1% in I_0, they are shifted by 6% in drive current.

believe that a more precise calculation, taking into account the single sideband modulation character found at the bifurcation, would yield a quantum-limited temperature $\hbar\omega_s/2k_B$. These calculations, which follow step-by-step the analysis of the SQUID [10], assume ideal matching to the noise impedance of the device, with components similar to those in conventional SQUID circuits. Although these results do not differ from those of the SQUID, the real advantage of our device lies in the spectral content of the total backaction noise, which is not contained in the usual definition of the noise temperature at ω_s. Since there is no on-chip dissipation, the only fluctuations contributing to the total backaction originate from our matched circulator load, within a band ω_p/Q centered at ω_p. In the SQUID, the total backaction consists of a wide spectrum extending from dc to several harmonics of the Josephson frequency. Efficient filtering over this wide band, leaving only the signal frequency unattenuated, is difficult. Moreover, it is easier in the JBA to fully thermalize [16] the requisite dissipation needed for amplification since it is completely in the off-chip circulator. Finally, the bifurcation amplifier does not suffer from quasiparticle generation associated with hysteretic SQUIDS [4] and dc current-biased junctions [2] that switch into the voltage state. Long quasiparticle recombination times at low temperatures limit the acquisition rate of these devices while the recombination process itself produces excess noise for adjacent circuitry [17].

In conclusion, we have developed a new amplification principle harnessing the nonlinear, nondissipative inductance of the Josephson junction to improve the performance of Josephson effect based amplifiers. The Josephson bifurcation amplifier is competitive with the SQUID for applications where low backaction is required. Its speed, suppression of on-chip dissipation, and latching make it ideal for the readout of superconducting qubits. At temperatures such that $T \leq 85$ mK, the discrimination power for quantronium would be greater than 95%, hence permitting stringent tests of quantum mechanics, like the violation of Bell's inequalities.

We would like to thank E. Boaknin, J. Clarke, M. Dykman, D. Esteve, S. Girvin, L. Grober, D. Prober, R. Schoelkopf, and D. Vion for discussions and assistance. This work was supported by the ARDA (ARO Grant No. DAAD19-02-1-0044), the NSF (ITR Grants No. DMR-0325580 and No. DMR-0072022), and the Keck Foundation.

[1] A. Aassime, G. Johansson, G. Wendin, R. J. Schoelkopf, and P. Delsing, Phys. Rev. Lett. **86**, 3376 (2001).
[2] D. Vion, A. Aassime, A. Cottet, P. Joyez, H. Pothier, C. Urbina, D. Esteve, and M. Devoret, Science **296**, 886 (2002).
[3] J. M. Martinis, S. Nam, J. Aumentado, and C. Urbina, Phys. Rev. Lett. **89**, 117901 (2002).
[4] I. Chiorescu, Y. Nakamura, C. J. P. M. Harmans, and J. E. Mooij, Science **299**, 1869 (2003).
[5] O. Buisson, F. Balestro, J. P. Pekola, and F. W. J. Hekking, Phys. Rev. Lett. **90**, 238304 (2003).
[6] T. V. Filippov, S. K. Tolpygo, J. Mannik, and J. E. Lukens, IEEE Trans. Appl. Supercond. **13**, 1005 (2003).
[7] A. B. Zorin, J. Exp. Theor. Phys. **98**, 1250 (2004).
[8] R. Tucker and M. J. Feldman, Rev. Mod. Phys. **57**, 1055 (1985).
[9] B. Yurke, L. R. Corruccini, P. G. Kaminsky, L. W. Rupp, A. D. Smith, A. H. Silver, R. W. Simon, and E. A. Whittaker, Phys. Rev. A **39**, 2519 (1989).
[10] J. Clarke, Proc. IEEE **77**, 1208 (1989).
[11] M. I. Dykman and M. A. Krivoglaz, Physica A (Amsterdam) **104**, 480 (1980).
[12] I. Siddiqi, R. Vijay, F. Pierre, C. M. Wilson, L. Frunzio, M. Metcalfe, C. Rigetti, R. J. Schoelkopf, M. H. Devoret, D. Vion, and D. E. Esteve, cond-mat/0312553.
[13] C. Urbina, D. Esteve, J. M. Martinis, E. Turlot, M. H. Devoret, H. Grabert, and S. Linkwitz, Physica B (Amsterdam) **169**, 26 (1991).
[14] A. Lupascu, C. J. M. Verwijs, R. N. Schouten, C. J. P. M. Harmans, and J. E. Mooij, Phys. Rev. Lett. **93**, 177006 (2004).
[15] M. Mück, J. B. Kycia, and J. Clarke, Appl. Phys. Lett. **78**, 967 (2001).
[16] F. C. Wellstood, C. Urbina, and J. Clarke, Appl. Phys. Lett. **54**, 2599 (1989).
[17] J. Mannik and J. E. Lukens, Phys. Rev. Lett. **92**, 057004 (2004).
[18] R. L. Kautz, Phys. Rev. A **38**, 2066 (1988).